doi.org/10.36721/PJPS.2022.35.6.SP.1827-1834.1

Cantharidin induces senescence via inhibition of AMP-activated protein kinase and activation of NLRP3 inflammasome in H9c2 cardiomyocytes

Yujing Shi[1], Yi Lv[2], Qi You[3] and Weidong Qian[1]*

[1]Department of Cardiovascular Diseases, Wujin Hospital of Traditional Chinese Medicine Affiliated to Nanjing University of Chinese Medicine, Wujin, China
[2]School of Basic Medicine, Shanghai University of Traditional Chinese Medicine, Shanghai, China
[3]School of Pharmacy, Nanjing University of Chinese Medicine, Nanjing, China

Abstract: Cantharidin is a natural compound with cardiotoxicity. Cellular senescence and senescence-associated secretory phenotype (SASP) are implicated in chemotherapy-associated cardiotoxicity. We here investigated how cantharidin induced cardiomyocyte senescence. H9c2 cells were treated with cantharidin. Senescence, mitochondrial functions, SASP, NOD-like receptor thermal protein domain associated protein 3 (NLRP3) signaling, and AMP-activated protein kinase (AMPK) phosphorylation were examined. Cantharidin inhibited viability and increased expression of senescence-associated β-galactosidase (SA-β-Gal), p16 and p21 in H9c2 cells, suggesting occurrence of senescence. Cantharidin impaired mitochondrial functions evidenced by reduction in basal respiration, ATP levels and spare respiratory capacity. Cantharidin also decreased mitochondrial DNA copy number and down-regulated mRNA levels of cytochrome c oxidase-I, -II and -III. Moreover, cantharidin suppressed activity of mitochondria complex-I and -II. Examinations of SASP showed that cantharidin promoted expression and secretion of SASP cytokines interleukin-1β, -6, and -8 and tumor necrosis factor-α, associated with activation of NLRP3/caspase-1 pathway. Finally, cantharidin suppressed AMPK phosphorylation. AMPK activator GSK621 abrogated the up-regulation of SA-β-Gal, p16 and p21 and counteracted the activation of NLRP3 and caspase-1 in cantharidin-challenged H9c2 cells. In conclusion, cantharidin stimulated senescence and SASP in cardiomyocytes through activation of NLRP3 inflammasome and inhibition of AMPK, providing novel molecular insights into cantharidin-induced cardiotoxicity.

Keywords: Cantharidin, senescence, SASP, NLRP3, AMPK.

INTRODUCTION

The dried body of cantharides has been utilized in traditional Chinese medicine for a long history. Cantharidin is one of the major components of the dried bodies of cantharides and is clinically used to treat rabies and dermatosis such as molluscum contagiosum and verruca vulgaris (Li *et al.* 2022). Nevertheless, inappropriate application of cantharidin may lead to adverse effects or toxicity, including dermatologic, gastrointestinal, cardiac, pulmonary and hematologic effects (Fabbro *et al.* 2022). These effects may result in poor prognoses and even multi-organ failure, limiting its legitimate medical purposes. There is clinical evidence that cantharidin poisoning can damage cardiovascular system and that the heart could be a major target organ of cantharidin at toxicological doses (Youyou *et al.* 2020; Zhang *et al.* 2020). Although cantharidin-caused heart damage has been reported, the underlying mechanisms remain to be uncovered. Understanding cantharidin-induced cardiotoxicity is important for developing strategies to prevent or reduce the potential myocardial damage when using cantharidin.

Cell senescence is a steady exit from cell cycle, contributing to tissue remodeling and injury response (Di Micco *et al.* 2021). Senescent cells become swelling and flattened, and overexpress the senescence marker senescence-associated β-galactosidase (SA-β-Gal). Concomitantly, cell cycle regulatory proteins p16 and p21 are highly expressed (Hu *et al.* 2022). More importantly, due to the alteration of genetic profiles in senescent cells, interleukins (ILs), tumor necrosis factor-α (TNF-α), growth factors and many other cytokines are secreted from the senescence cells, that is, the senescence-associated secretory phenotype (SASP) occurs, disrupting tissue functions (Kumari *et al.* 2021). In the heart, it is recognized that the cardiomyocytes as terminus-differentiated cells generally exhibit declines of various functions when undergoing senescence, including hypertrophic growth, contractile abnormality, mitochondria dysfunction and SASP (Chen *et al.* 2022; Mehdizadeh *et al.* 2022). In particular, mitochondrial fission–fusion imbalance is a key characteristic of cardiomyocyte senescence and restoration of mitochondrial function through regulating dynamin-related protein 1 (Drp1)/Parkin pathway can inhibit cardiomyocyte senescence (Nishimura *et al.* 2018). Moreover, the SASP cytokines are critical for regulating the heart microenvironment, contributing to cardiac dysfunction (Tang *et al.* 2020).

**Corresponding author:* e-mail: qianweidong88@yeah.net

It is recognized that cellular senescence can be a response to a range of intrinsic and extrinsic insults (Di Micco *et al.* 2021). Mounting evidence suggests that induction of senescence of cardiomyocytes is involved in the cardiotoxicity induced by doxorubicin and other anthracycline chemotherapeutic drugs (Russo *et al.* 2021). Cantharidin has been demonstrated to stimulate programmed cell death such as apoptosis and autophagy under various pathophysiological conditions (Liu *et al.* 2020; He *et al.* 2022). We here investigated whether cantharidin could induce senescence of cardiomyocytes and elucidated the underlying mechanism in the hope of understanding the molecular basis of the cardiotoxicity of cantharidin.

MATERIALS AND METHODS

Cell line and chemicals

The H9c2 cell line was provided by Cell Bank of Type Culture Collection of Chinese Academy of Sciences (Shanghai, China). H9c2 cell line was maintained in Dulbecco's Minimum Essential Medium (DMEM) with fetal bovine serum (FBS) of 10% concentration, penicillin at 100 U/ml, and streptomycin at 100 mg/ml. H9c2 cell line was grown in an incubator at 37˚C containing 5% CO_2 and 95% air. H9c2 cell line was treated with cantharidin (purity ⩾ 98.0%; Sigma-Aldrich, Shanghai, China) and the compound GSK621 (purity ⩾ 98.0%; Sigma-Aldrich, Shanghai, China) at indicated concentrations. Cantharidin and GSK621 were dissolved with dimethylsulfoxide (DMSO) and DMSO alone was set as the negative control.

Measurement of H9c2 cell viability

The viability of H9c2 cells upon cantharidin treatment was detected using the Cell Counting Kit-8 (CCK-8) assay. H9c2 cells at a density of $1x10^5$/ml were grown in 96-well plates. Then, 100 µl DMEM containing FBS (10%) was added to every single well, which were then incubated with cantharidin of different concentrations for 24 h. Next, the CCK-8 reagent at a concentration of 10 µl/well was added following incubation for a 2 h time duration at 37˚C. Spectrophotometric absorbance (450 nm) was determined by a microplate spectrophotometer. The viability of cantharidin-treated H9c2 cells is expressed as the percentages of the control cells.

Lactate dehydrogenase (LDH) release assay

The H9c2 cells at a density of $1x10^5$/ml were cultured in 96-well plates. Next, the H9c2 cells were treated with cantharidin of different concentrations for 24 h. The cell supernatants were collected for analysis of LDH release. The LDH reagents provided by Nanjing Jiancheng Bioengineering Institute (Nanjing, China) were incubated with the collected cell supernatant for a 1.5h time duration. Spectrophotometric absorbance (450 nm) was detected using a microplate spectrophotometer. Values are expressed as fold of control.

Staining of senescence marker SA-β-Gal

H9c2 cell line was treated with cantharidin or GSK621 for 24 h at indicated concentrations. Staining with SA-β-Gal was performed using the Kits (Beyotime Biotechnology, Shanghai, China) based on the instructions. In brief, the treated H9c2 cells were incubated with 0.5% glutaraldehyde for 15 min, and phosphate buffered saline was used to wash the cells. Next, the treated H9c2 cells were stained overnight. Random views were taken by a light microscope blindly. Representative views are shown.

Analysis of mitochondrial oxygen consumption rate (OCR)

H9c2 cell line was grown in XF24-well plates (Seahorse Bioscience, Massachusetts, USA) at a density of $1x10^4$/well, followed by treatment with cantharidin at indicated concentrations. Cell medium was changed with bicarbonate-free assay medium and low-buffered composed by glucose at 10 mM, pyruvate at 1 mM, and L-glutamine at 2 mM. An XF24 Extracellular Flux Analyzer (Seahorse Bioscience, Massachusetts, USA) was used to analyze the OCR based on the procedures provided by the manufacture. The basal respiration was determined firstly in an unbuffered medium. Thereafter, 1 µM oligomycin was added to inhibit the production of mitochondrial ATP, making the cells use glycolysis to produce ATP. Next, the uncoupler FCCP of 2 µM was used to analyze the maximal respiration and respiratory reserve capacity. Finally, rotenone at 0.5 µM and antimycin A at 0.5 µM were used to inhibit the activity of complex-I and complex-III for completely blocking the mitochondrial oxygen consumption. The three reagents were added serially to detect the synthesis of ATP, the maximal respiration, and the non-mitochondrial respiration. The spare respiratory capacity was measured based on the above parameters and the basal respiration.

Measurement of mitochondrial DNA (mtDNA) copy number

H9c2 cell line was treated with cantharidin of different concentrations for 24 h. Next, total DNA was prepared using the FlexiGene DNA Kits (Qiagen, Hilden, Germany) following the instructions provided by the manufacturer. The DNA concentration was quantified spectrophotometrically at 260 nm followed by real-time PCR on the iQ5 system provided by Bio-Rad Laboratories (Hercules, USA). Nicotinamide adenine dinucleotide dehydrogenase subunit 1 (ND1; F: 5'-CCTCCCATTCATTATCGCCGCCCTTGC-3', R: 5'-GTCTGGGTCTCCTAGTAGGTCTGGGAA-3') was utilized for amplification of mtDNA, and lipoprotein lipase (LPL) was used as the internal control. The mtDNA copy number is represented by the ddCT (ND1/LPL).

Measurement of mitochondrial complex-I and complex-III activity

H9c2 cell line was treated with cantharidin of different

concentrations for 24 h. For measurement of the activity of mitochondrial complex-I, mitochondrial fraction of 1 μg was added to 100μl NADH dehydrogenase reaction buffer in 96-well plates followed by 10 min incubation at room temperature. Thereafter, 200μM NADH was added to every well to initiate the assay reaction, and the absorbance (340 nm) was detected. For measurement of the mitochondrial complex-III activity, mitochondrial fraction of 0.5μg was added to 100μl cytochrome c reductase reaction buffer in 96-well plates followed by 10 min incubation at room temperature. Then, 50μM of oxidized cytochrome c was used to start the assay reaction, and the absorbance (550 nm) was detected. Values are expressed as fold of control.

Enzyme-linked immunesorbent assay (ELISA)

The levels of SASP cytokines in the H9c2 cell supernatant treated with cantharidin of different concentrations for 24 h were detected using ELISA Kits purchased from Nanjing Jiancheng Bioengineering Institute (Nanjing, China) based on the manufacture's protocols. Spectrophotometric absorbance (450 nm) was detected using a microplate spectrophotometer.

Real-time PCR

H9c2 cell line was treated with cantharidin or GSK621 of different concentrations for 24 h. Total RNA of the treated cells was prepared using the Trizol reagent obtained from Invitrogen (Carlsbad, USA). The total RNA of 1 μg was used to synthesize the first-strand cDNA using the PrimeScript RT Kits purchased from TakaraBio (Tokyo, Japan) in accordance with the manufacture's protocols. Real-time PCR analysis was performed on the iQ5 system provided by Bio-Rad Laboratories (Hercules, USA). The SYBR Green I dye master at 7.5 μl, forward primers at 2 pM, and reverse primers at 2 pM were contained in the reaction mixtures. The thermocycle conditions were set as denaturation for 10 min duration at 50°C and 95°C, and 40 cycles at 95°C for 15 s and 60°C for 1 min. The relative expression of mRNA of target genes was calculated using glyceraldehyde phosphate dehydrogenase (GAPDH) as the invariant control based the $2^{-\Delta\Delta CT}$ method. The primer sequences of target genes (GenScript, Nanjing, China) were presented as follows: p16 (F: 5'-ATCTCCGAGAGGAAGGCGAACTCG-3', R: 5'-TCTGTCCCTCCCTCCCTCTGCTAAC-3'); p21 (F: 5'-TGTTCCACACAGGAGCAAAG-3', R: 5'-AACACGCTCCCAGACGTAGT-3'); COX-I (F: 5'-TGACACCTCATATTGTATTCCCCC-3', R: 5'-TTTCGCTGCCACATCACTTG-3'); COX-II (F: 5'-AAGGGATTGTTGCGGTGCTA-3', R: 5'-TGCCCAATATCCCGTGCATT-3'); COX-III (F: 5'-AGAAAAGGTGGCTGTGAGAGG-3', R: 5'-GGTCATACTTGGCCCACCC-3'); GAPDH (F: 5'-GCATCTTCTTGTGCAGTGCC-3', R: 5'-GATGGTGATGGGTTTCCCGT-3').

Western blotting

H9c2 cell line was treated with cantharidin or GSK621 of different concentrations for 24 h. Whole cell proteins of the treated cells were isolated using the radioimmunoprecipitation analysis buffer plus protease inhibitors and phosphatase inhibitors, and the BCA Kits provided by Pierce (USA) were used to detect protein concentrations. Proteins of 50 μg/well were uploaded and separated on SDS-polyacrylamide gel through electrophoresis. The separated proteins were transferred to PVDF membranes purchased from Millipore (Burlington, USA). The transferred membranes were incubated with TBS-T solution containing 5% skim milk. The primary antibodies against p21, p16, TNF-α, IL-1β, IL-8, IL-6, NLRP3, cleaved-caspase-1, p-AMPK, AMPK and GAPDH, and the horseradish peroxidase-conjugated secondary antibodies (Cell Signaling Technology, USA) were used to monitor the target proteins followed by visualization. The GAPDH was used for confirming the equivalent loading of target proteins, which were quantified using the Image Lab Software and are expressed as fold of control. Representative blots are presented.

STATISTICAL ANALYSES

All data are shown as the mean ± standard deviation (SD). The GraphPad Prism software (version 9.3.1) was utilized for statistical analyses of the data. Statistical differences between multiple groups were determined by the one- way analysis of variance followed by the Tukey's post-hoc test. Value of $P<0.05$ was set to be significantly different.

RESULTS

Cantharidin induces senescence in H9c2 cells

How cantharidin affected the H9c2 cell viability was evaluated. The CCK-8 assays showed that cantharidin reduced H9c2 cell viability concentration-dependently, and that cantharidin at 5μM or larger concentrations led to significant inhibitory effects (fig. 1A). Accordingly, cantharidin at 5, 10, and 20μM was used for subsequent experiments. LDH release assays revealed that cantharidin at these concentrations did not cause significant extra cellular LDH leakage in H9c2 cells, suggesting that cell membrane rupture and necrosis were not involved in cantharidin effects (fig. 1B). We next explored whether cellular senescence was involved in the current context. Interestingly, cantharidin increased the expression of SA-β-Gal concentration-dependently in H9c2 cells (fig. 1C), and the expression of p16 and p21, two key biomarkers of cellular senescence (Ogrodnik 2021), was also up-regulated by cantharidin at both mRNA and protein levels (fig. 1D, E), suggesting the occurrence of senescence. Collectively, these results revealed that cantharidin stimulated senescence in H9c2 cells.

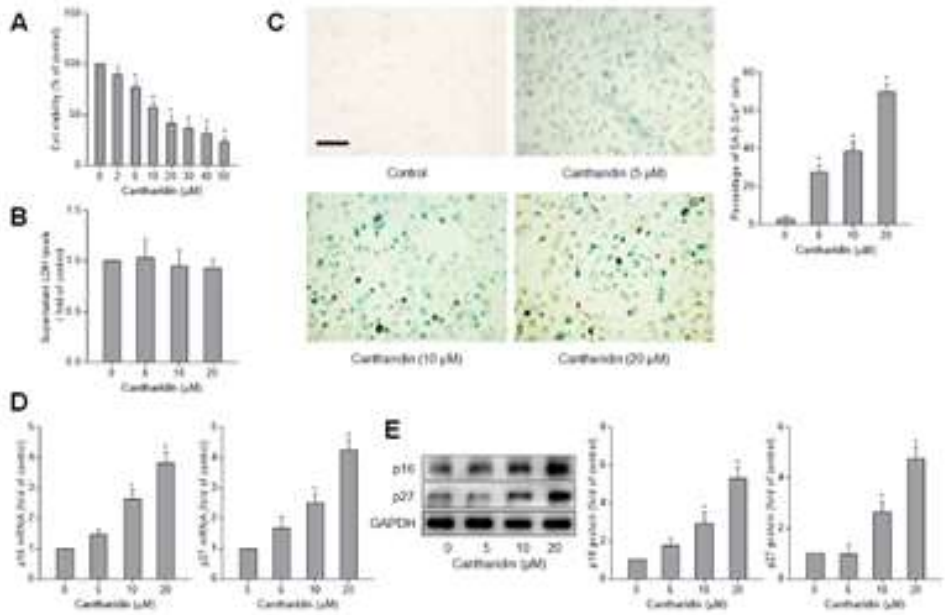

Fig. 1: Cantharidin induces senescence in H9c2 cells. H9c2 cells were treated with cantharidin at indicated concentrations for 24h. (a) CCK-8 assay for detecting cell viability. Cell viability is expressed as percentages of control. **P*<0.05 versus control. (b) LDH release assay for evaluating cytotoxicity. Values are expressed as fold of control. **P*< 0.05 versus control. (c) SA-β-Gal staining. Positive SA-β-Gal staining indicates the senescent cells. Scale bar 50μm. (d) Real-time PCR analysis of senescence markers p16 and p21. Relative mRNA expression is expressed as fold of control after normalization to GAPDH. **P*<0.05 versus control. (e) Western blot analysis of senescence markers p16 and p21 with quantification. Relative protein expression is expressed as fold of control after normalization to GAPDH. **P*<0.05 versus control.

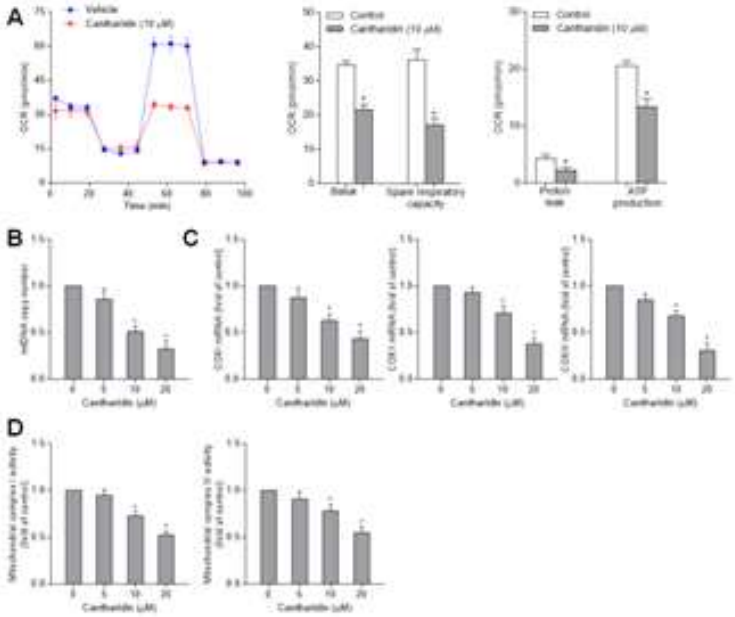

Fig. 2: Cantharidin impairs mitochondrial functions in H9c2 cells. H9c2 cells were treated with cantharidin at indicated concentrations for 24h, or at 10μM for indicated time duration. (a) Measurement of mitochondrial OCR. The basal levels, spare respiratory capacity, proton leak and ATP levels were calculated. **P*<0.05 versus control. (b) Real-time PCR analysis of mtDNA copy number. **P*<0.05 versus control. (c) Real-time PCR analysis of mtDNA-encoded subunits COX-I, COX-II and COX-III. Relative mRNA expression is expressed as fold of control after normalization to GAPDH. **P*<0.05 versus control. (d) Measurement of activity of mitochondrial complex-I and complex-II. Values are expressed as fold of control. **P*<0.05 versus control.

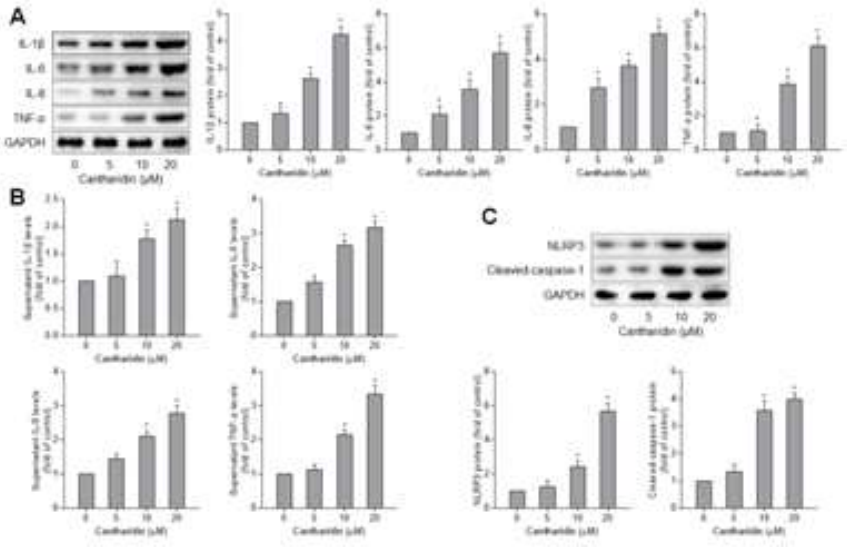

Fig. 3: Cantharidin promotes SASP associated with activation of NLRP3 inflammasome in H9c2 cells. H9c2 cells were treated with cantharidin at indicated concentrations for 24h. (a) Western blot analysis of SASP cytokines IL-1β, IL-6, IL-8 and TNF-α with quantification. Relative protein expression is expressed as fold of control after normalization to GAPDH. **P*<0.05 versus control. (b) ELISA for detecting the supernatant levels of IL-1β, IL-6, IL-8 and TNF-α. **P*<0.05 versus control. (c) Western blot analysis of NLRP3 and cleaved-caspase-1 with quantification. Relative protein expression is expressed as fold of control after normalization to GAPDH. **P*<0.05 versus control.

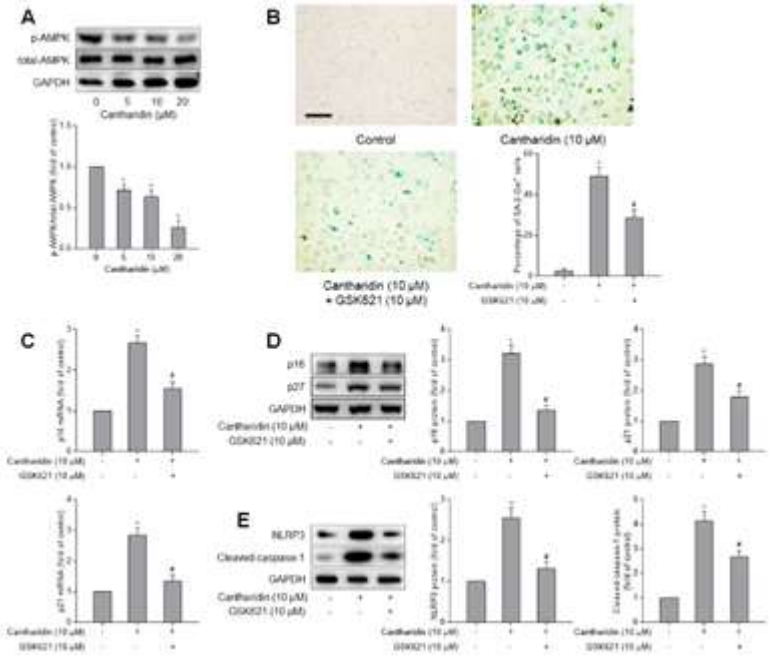

Fig. 4: Inhibition of AMPK is required for cantharidin to induce senescence and activate NLRP3 inflammasome in H9c2 cells. H9c2 cells were treated with cantharidin and/or GSK621 at indicated concentrations for 24h. (a) Western blot analysis of phosphorylation of AMPK with quantification. Relative p-AMPK levels are expressed as fold of control after normalization to total-AMPK. **P*<0.05 versus control. (b) SA-β-Gal staining. Positive SA-β-Gal staining indicates the senescent cells. Scale bar 50μm. (c) Real-time PCR analysis of senescence markers p16 and p21. Relative mRNA expression is expressed as fold of control after normalization to GAPDH. **P*<0.05 versus control, $^{\#}P$<0.05 versus cantharidin. (d) Western blot analysis of senescence markers p16 and p21 with quantification. Relative protein expression is expressed as fold of control after normalization to GAPDH. **P*<0.05 versus control, $^{\#}P$<0.05 versus cantharidin. (e) Western blot analysis of NLRP3 and cleaved-caspase-1 with quantification. Relative protein expression is expressed as fold of control after normalization to GAPDH. **P*<0.05 versus control, $^{\#}P$<0.05 versus cantharidin.

Cantharidin impairs mitochondrial functions in H9c2 cells

We next investigated how cantharidin stimulated H9c2 cell senescence focusing on mitochondrial functions, because mitochondria play a key role in cellular senescence (Martini *et al.* 2022). Examinations of mitochondrial OCR showed that the basal respiration, the ATP contents, the spare respiratory capacity and the maximal respiration were all significantly reduced in cantharidin-treated H9c2 cells (fig. 2A). Given that mtDNA is a sensitive maker for mitochondrial function (Aretz *et al.* 2020), we detected it and found that the copy number of mtDNA in cantharidin-treated H9c2 cells was lowered significantly (fig. 2B). The changes of mtDNA-encoded genes were also examined, because they are important for mitochondrial functions (Aretz *et al.* 2020). The obtained results demonstrated that the transcript levels of cytochrome c oxidase subunit (COX)-I, -II and -III were all decreased significantly in cantharidin-stimulated H9c2 cells (fig. 2C). Moreover, cantharidin reduced the activity of mitochondria complex-I and -II concentration-dependently in H9c2 cells (fig. 2D). In aggregate, the above observations revealed that cantharidin promoted mitochondrial dysfunction in H9c2 cells.

Cantharidin promotes SASP associated with activation of NOD-like receptor thermal protein domain associated protein 3 (NLRP3) inflammasome in H9c2 cells

Secretion of SASP pro-inflammatory cytokines is an important feature of senescent cells (Kumari *et al.* 2021). We examined a series of inflammatory cytokines in H9c2 cells upon cantharidin treatment. The protein contents of IL-1β, -6 and -8, and TNF-α were elevated by cantharidin in H9c2 cells (fig. 3A). Consistently, their concentrations in the supernatant were all increased in cantharidin-treated H9c2 cells, indicating abundant extracellular secretion of inflammatory cytokines (fig. 3B). Given that the NLRP3 inflammasome is a master hub of inflammatory cytokine synthesis (Xu *et al.* 2022), we examined the effects of cantharidin on the NLRP3/caspase-1 pathway. As expected, cantharidin increased the protein abundance of NLRP3 and the cleaved form of caspase-1 concentration-dependently in H9c2 cells, suggesting the activation of NLRP3 inflammasome (fig. 3C). Collectively, these data revealed that cantharidin promoted SASP in H9c2 cells, which was correlated with activation of NLRP3/caspase-1 signaling.

Inhibition of AMP-activated protein kinase (AMPK) is required for cantharidin induction of senescence and activation of NLRP3 inflammasome in H9c2 cells

Finally, we explored the role of AMPK in cantharidin induction of H9c2 cell senescence, because this kinase governs cellular homeostasis and cell fate under a variety of pathophysiological circumstances (Trefts *et al.* 2021). We found that the phosphorylation of AMPK was concentration-dependently suppressed by cantharidin in H9c2 cells (fig. 4A). The specific AMPK activator GSK621 (Ting-Ting *et al.* 2019) was used to test whether the effects of cantharidin were dependent on inhibition of AMPK. SA-β-Gal staining showed that GSK621 significantly abolished cantharidin-elevated SA-β-Gal expression in H9c2 cells (fig. 4B). Meanwhile, cantharidin up-regulation of p16 and p21 was abrogated by GSK621 in H9c2 cells (fig. 4C and D). Furthermore, GSK621 considerably counteracted the activation of NLRP3 and caspase-1 in cantharidin-challenged H9c2 cells (fig. 4E). In aggregate, our findings indicated that inhibition of AMPK is required for cantharidin to stimulate senescence and to activate the NLRP3 signaling in H9c2 cells.

DISCUSSION

Cellular senescence and the release of SASP molecules have been implicated in cardiac pathologies including myocardial infarction and ischaemia, heart failure and chemotherapy-associated cardiotoxicity (Mehdizadeh *et al.* 2022). Cancer chemotherapeutic drugs, especially doxorubicin, have been demonstrated to cause senescence in many types of cardiovascular cells, associated with serious dose-limiting cardiotoxicity (Andreou *et al.* 2022). Doxorubicin-induced cardiomyocyte senescence can lead to cardiac remodeling and dysfunction (Wen *et al.* 2021). Therefore, understanding of how cardiomyocyte senescence is regulated may facilitate the development of protective approaches and prevent the occurrence of cardiotoxicity when using cancer chemotherapeutics.

The natural compound cantharidin has increasingly been shown to possess antitumor effects (Ren *et al.* 2021), which were associated with suppression of protein phosphatase 1 and protein phosphatase type 2A (Pan *et al.* 2019). In the following extensive studies, cantharidin was demonstrated to inhibit colon, bladder, breast, pancreatic, and liver cancers (Naz *et al.* 2020). In the current study, after we ruled out the involvement of necrosis in cantharidin effects, we observed that cantharidin effectively induced senescence in H9c2 cardiomyocytes evidenced by SA-β-Gal positive staining and elevated expression of p21 and p27. To the best of our knowledge, the present study was the first investigation of cantharidin-induced senescence in eukaryotic cells, offering new evidence for the cardiotoxicity caused by cantharidin. Although senescence is recognized as a response to cell cycle arrest unique to dividing cells, it may be a more common response to cellular stress occurring in post-mitotic cells such as cardiomyocytes (Sapieha *et al.* 2018; von Zglinicki *et al.* 2021). Senescent cardiomyocytes are thought to be characterized by persistent DNA injury, which may be due to mitochondrial dysfunction and by up-regulation of classical markers p16, p21 and p53 (Anderson *et al.* 2019). Consistently, our current data demonstrated that

cantharidin-treated H9c2 cardiomyocytes exhibited a deterioration of mitochondrial functions accompanied by increased levels of SA-β-Gal, p16 and p21. Furthermore, we measured the mitochondrial OCR to monitor the functional alterations, indicating that cantharidin-induced senescence reduced the basal respiration, ATP contents, and spare respiratory capacity. These could increase mtDNA mutation and impair mitochondrial complex activity. We speculated that cantharidin-induced mitochondrial dysfunction in cardiomyocytes could result in abnormality of extracellular environment maintenance, affecting cardiac functions.

Compelling evidence suggests that the senescent cells exhibit a complex SASP involving a group of pro-inflammatory cytokines with critical autocrine and paracrine effects on cells and tissues (Mehdizadeh *et al.* 2022). It has been reported that the SASP components secreted by the senescent cardiomyocytes include ILs, TNF-α, TGF-β, monocyte chemoattractant protein-1, etc., which play key roles in modulation of non-myocytes within heart microenvironment, contributing to cardiac dysfunction and remodeling (Tang *et al.* 2020). In the current work, we found significant production of ILs and TNF-α in cantharidin-treated cardiomyocytes. These inflammatory cytokines were consistently reported to be secreted by the senescent cardiomyocytes in a recent study to understand the importance of senescence in the pathology of atrial fibrillation (Adili *et al.* 2022). Next, we discovered that cantharidin activated the NLRP3 inflammasome pathway in H9c2 cardiomyocytes. Recent investigations have linked the NLRP3 inflammasome to cellular senescence and shown that pharmacological blockade of NLRP3 signaling could mitigate senescence in various cell types (Tai *et al*. 2022; Valencia *et al.* 2022). A recent interesting study revealed that NLRP3 inflammasome activation was involved in doxorubicin-induced cardiomyocyte senescence (Huang *et al*. 2020), which was validated by our current results in the context of cantharidin treatment. Of note, doxorubicin-induced NLRP3 activation and cardiomyocyte senescence was identified to be dependent on thioredoxin-interactive protein in that study (Huang *et al.* 2020). However, our data here highlighted that suppression of AMPK activation was required for cantharidin-induced NLRP3 activation and senescence in cardiomyocytes. Consistently, there have been many studies demonstrating that AMPK was inactivated in cellular senescence under various pathophysiological circumstances and that pharmacological activation of AMPK could repress senescence-associated pathways (Chen *et al.* 2021; Kim *et al.* 2021; Du *et al.* 2022). Taken these recognitions together, we postulated that AMPK could be a target molecule for controlling cardiomyocyte senescence and that AMPK agonists could serve as a therapeutic option for counteracting cardiotoxicity of cantharidin.

CONCLUSION

Cantharidin stimulated senescence and SASP in H9c2 cardiomyocytes through inhibition of AMPK and activation of NLRP3 inflammasome signaling. These data highlighted senescence and related pathway as key mediators of cantharidin-induced cardiotoxicity, providing novel prophylactic and/or therapeutic approaches to overcome cardiotoxic effects of cantharidin in clinical application.

ACKNOWLEDGMENTS

This work was supported by the Natural Science Foundation of Nanjing University of Chinese Medicine (XZR2020092)**.**

REFERENCES

Adili A, Zhu X, Cao H, Tang X, Wang Y, Wang J, Shi J, Zhou Q and Wang D (2022). Atrial fibrillation underlies cardiomyocyte senescence and contributes to deleterious atrial remodeling during disease progression. *Aging Dis*., **13**(1): 298-312.

Anderson R, Lagnado A, Maggiorani D, Walaszczyk A, Dookun E, Chapman J, Birch J, Salmonowicz H, Ogrodnik M, Jurk D, Proctor C, Correia-Melo C, Victorelli S, Fielder E, Berlinguer-Palmini R, Owens A, Greaves LC, Kolsky KL, Parini A, Douin-Echinard V, LeBrasseur NK, Arthur HM, Tual-Chalot S, Schafer MJ, Roos CM, Miller JD, Robertson N, Mann J, Adams PD, Tchkonia T, Kirkland JL, Mialet-Perez J, Richardson GD and Passos JF (2019). Length-independent telomere damage drives post-mitotic cardiomyocyte senescence. *EMBO J*. **38**(5): e100492.

Andreou C and Matsakas A (2022). Current insights into cellular senescence and myotoxicity induced by doxorubicin: The role of exercise and growth factors. *Int. J. Sports Med*., **43**(13): 1084-1096.

Aretz I, Jakubke C and Osman C (2020). Power to the daughters - mitochondrial and mtDNA transmission during cell division. *Biol Chem*., **401**(5): 533-546.

Chen M, Zhang C, Zhou N, Wang X, Su D and Qi Y (2021). Metformin alleviates oxidative stress-induced senescence of human lens epithelial cells via AMPK activation and autophagic flux restoration. *J. Cell Mol Med*., **25**(17): 8376-8389.

Chen MS, Lee RT and Garbern JC (2022). Senescence mechanisms and targets in the heart. *Cardiovasc Res*., **118**(5): 1173-1187.

Di Micco R, Krizhanovsky V, Baker D and d'Adda di Fagagna F (2021). Cellular senescence in ageing: from mechanisms to therapeutic opportunities. *Nat Rev Mol Cell Biol*., **22**(2): 75-95.

Du J, Xu M, Kong F, Zhu P, Mao Y, Liu Y, Zhou H, Dong Z, Yu Z, Du T, Gu Y, Wu X, Geng D and Mao H (2022). CB2R Attenuates intervertebral disc degeneration by

delaying nucleus pulposus cell senescence through AMPK/GSK3beta Pathway. *Aging Dis*., **13**(2): 552-567.

Fabbro SK and Stoff BK (2022). Ethical issues of compounding cantharidin in dermatology. *J Am Acad Dermatol*. (In Press).

He T, Wang Q, Ao J, Chen K, Li X, Zhang J and Duan C (2022). Endoplasmic reticulum stress contributes to autophagy and apoptosis in cantharidin-induced nephrotoxicity. *Food Chem Toxicol*., **163**(5): 112986.

Hu L, Li H, Zi M, Li W, Liu J, Yang Y, Zhou D, Kong QP, Zhang Y and He Y (2022). Why senescent cells are resistant to apoptosis: An insight for senolytic development. *Front Cell Dev Biol*., **10**(2): 822816.

Huang PP, Fu J, Liu LH, Wu KF, Liu HX, Qi BM, Liu Y and Qi BL (2020). Honokiol antagonizes doxorubicininduced cardiomyocyte senescence by inhibiting TXNIPmediated NLRP3 inflammasome activation. *Int. J. Mol. Med*., **45**(1): 186-194.

Kim D, Yang KE, Kim DW, Hwang HY, Kim J, Choi JS and Kwon HJ (2021). Activation of Ca(2+) -AMPK-mediated autophagy by ginsenoside Rg3 attenuates cellular senescence in human dermal fibroblasts. *Clin Transl Med*., **11**(8): e521.

Kumari R and Jat P (2021). Mechanisms of cellular senescence: Cell cycle arrest and senescence associated secretory phenotype. *Front Cell Dev. Biol*., **9**: 645593.

Li S, Wu X, Fan G, Du K and Deng L (2022). Exploring cantharidin and its analogues as anticancer agents: A review. *Curr Med Chem*. (In Press).

Liu F, Duan C, Zhang J and Li X (2020). Cantharidin-induced LO2 cell autophagy and apoptosis via endoplasmic reticulum stress pathway *in vitro*. *J Appl Toxicol*., **40**(12): 1622-1635.

Martini H and Passos JF (2022). Cellular senescence: All roads lead to mitochondria. *FEBS J*. (In Press).

Mehdizadeh M, Aguilar M, Thorin E, Ferbeyre G and Nattel S (2022). The role of cellular senescence in cardiac disease: Basic biology and clinical relevance. *Nat. Rev. Cardiol*., **19**(4): 250-264.

Naz F, Wu Y, Zhang N, Yang Z and Yu C (2020). Anticancer attributes of cantharidin: Involved molecular mechanisms and pathways. *Molecules*. **25**(14): 3279.

Nishimura A, Shimauchi T, Tanaka T, Shimoda K, Toyama T, Kitajima N, Ishikawa T, Shindo N, Numaga-Tomita T, Yasuda S, Sato Y, Kuwahara K, Kumagai Y, Akaike T, Ide T, Ojida A, Mori Y and Nishida M (2018). Hypoxia-induced interaction of filamin with Drp1 causes mitochondrial hyperfission-associated myocardial senescence. *Sci Signal*., **11**(556).

Ogrodnik M (2021). Cellular aging beyond cellular senescence: Markers of senescence prior to cell cycle arrest *in vitro* and *in vivo*. *Aging Cell*. **20**(4): e13338.

Pan Y, Zheng Q, Ni W, Wei Z, Yu S, Jia Q, Wang M, Wang A, Chen W and Lu Y (2019). Breaking glucose transporter 1/pyruvate kinase M2 glycolytic loop is required for cantharidin inhibition of metastasis in highly metastatic breast cancer. *Front Pharmacol*., **10**(5): 590.

Ren Y and Kinghorn AD (2021). Antitumor potential of the protein phosphatase inhibitor, cantharidin and selected derivatives. *Bioorg Med. Chem*., **32**(4): 116012.

Russo M, Bono E and Ghigo A (2021). The interplay between autophagy and senescence in anthracycline cardiotoxicity. *Curr. Heart Fail. Rep*., **18**(4): 180-190.

Sapieha P and Mallette FA (2018). Cellular senescence in postmitotic cells: Beyond growth arrest. *Trends Cell Biol*., **28**(8): 595-607.

Tai GJ, Yu QQ, Li JP, Wei W, Ji XM, Zheng RF, Li XX, Wei L and Xu M (2022). NLRP3 inflammasome links vascular senescence to diabetic vascular lesions. *Pharmacol. Res*., **178**(4): 106143.

Tang X, Li PH and Chen HZ (2020). Cardiomyocyte senescence and cellular communications within myocardial microenvironments. *Front Endocrinol (Lausanne)*. **11**(5): 280.

Ting-Ting L, Yuan G, Jun L, Dan X and Hong-Bo T (2019). GSK621 attenuates oxygen glucose deprivation/re-oxygenation-induced myocardial cell injury via AMPK-dependent signaling. *Biochem Biophys. Res. Commun*., **514**(3): 826-834.

Trefts E and Shaw RJ (2021). AMPK: restoring metabolic homeostasis over space and time. *Mol Cell*., **81**(18): 3677-3690.

Valencia I, Vallejo S, Dongil P, Romero A, San Hipolito-Luengo A, Shamoon L, Posada M, Garcia-Olmo D, Carraro R, Erusalimsky JD, Romacho T, Peiro C and Sanchez-Ferrer CF (2022). DPP4 promotes human endothelial cell senescence and dysfunction via the PAR2-COX-2-TP axis and NLRP3 inflammasome activation. *Hypertension*. **79**(7): 1361-1373.

von Zglinicki T, Wan T and Miwa S (2021). Senescence in post-mitotic cells: A driver of aging? *Antioxid Redox Signal*., **34**(4): 308-323.

Wen Y, Shen F and Wu H (2021). Role of C5a and C5aR in doxorubicin-induced cardiomyocyte senescence. *Exp Ther Med*., **22**(4): 1114.

Xu J and Nunez G (2022). The NLRP3 inflammasome: activation and regulation. *Trends Biochem Sci*., (in Press).

Youyou Z, Yalei Y, Jie Z, Chuhuai G, Liang L and Liang R (2020). Molecular biomarkers of cantharidin-induced cardiotoxicity in Sprague-Dawley rats: Troponin T, vascular endothelial growth factor and hypoxia inducible factor-1alpha. *J. Appl. Toxicol*., **40**(8): 1153-1161.

Zhang Y, Liu L and Ren L (2020). RNA-sequencing-based transcriptome analysis of cantharidin-induced myocardial injury. *J. Appl Toxicol*., **40**(11): 1491-1497.